

Sustainable Cooperative Communication in Wireless Powered Networks With Energy Harvesting Relay

Zhao Chen¹, Lin X. Cai, *Member, IEEE*, Yu Cheng, *Senior Member, IEEE*, and Hanguan Shan, *Member, IEEE*

Abstract—In this paper, we consider a fully sustainable cooperative communication system which consists of multiple source nodes with radio-frequency (RF) energy harvesting capabilities, a half-duplex relay node with renewable energy supplies, and a destination node. Specifically, the relay node is powered by the green energy harvested from renewable sources such as solar or wind, while the source nodes are wirelessly charged by the RF energy from the relay node's forwarding signals to the destination node. An optimal joint time scheduling and power allocation problem is formulated to achieve the maximum system sum-throughput of the users over a finite time horizon. To tackle the formulated NP-hard non-convex mixed integer nonlinear programming problem, we first analyze its upper bound by problem reformulation and relaxation, which can be simplified by the directional water filling algorithm and iteratively solved by sequential parametric convex approximation. We then propose an optimal branch-and-bound framework to solve the formulated problem, and develop an efficient sub-optimal offline algorithm and a heuristic online algorithm to reduce the computational complexity. Finally, extensive simulations are conducted to verify the superiority of the proposed solution and demonstrate that the sub-optimal algorithm approaches the performance upper bound with polynomial time complexity.

Index Terms—Energy harvesting, wireless information and power transfer, buffer-aided relaying, sustainable communication, time scheduling, power allocation.

I. INTRODUCTION

AS THE rapid growing of energy consumption for the ever-increasing demand of ubiquitous broadband wireless communication services, green energy technologies have been continuously studied to construct sustainable and environmentally friendly communication systems [1]. Recently, energy harvested from renewable energy sources, e.g., solar and wind, emerges as an attractive alternative for traditional

on-grid power from burning fossil fuels [2]–[5], which are free for users and can relieve the global warming effect by decreasing the emission of greenhouse gases. However, due to the intermittent nature of renewable sources, such energy harvested from the surrounding environment are dynamically changing with uncertain timing and quantity. Thus, to maintain sustainability and improve system throughput, energy harvesting (EH) techniques [6] have been proposed to tackle random energy arrivals of renewable sources and efficiently utilize the available energy for wireless transmissions.

EH based wireless communications have been extensively studied. For point-to-point scenario, throughput maximization for Gaussian channels [7], [8] and fading channels [9] are considered, where the directional water filling (DWF) algorithm was proposed to allocate optimal transmission powers for each time slot in the offline problem. Then, cooperative communications with EH were investigated in [10]–[12]. Given an EH source and a non-EH half-duplex relay, throughput maximization and transmission time minimization were studied in [10]. Moreover, the system with both EH source and EH relay was considered in [11]. Joint time scheduling and power allocation is optimized for continuous time systems in [10] and [11]. For time slotted systems [12], only transmission power was optimized for Gaussian relay channel, where both the source and relay nodes are also EH enabled.

Meanwhile, wireless power transfer (WPT) has drawn increasing interests for energy-constrained wireless networks in recent years [13]. It aims to charge low-power devices with dedicated wireless signals and thus prolong their lifetime. As a result, wireless powered communication networks (WPCNs) have attracted a lot of attentions [14]–[17]. In a WPCN, the harvest-then-transmit protocol is commonly applied to charge single [14] or multiple [15] wireless powered devices in the downlink, and then the devices can transmit information with the harvested radio-frequency (RF) energy in the uplink. With jointly optimized power level and time duration, RF energy signals will be transferred by either a dedicated energy access point (E-AP) [16] or a hybrid access point (H-AP) [15] which is integrated with a traditional data AP. As for APs equipped with multi-antennas, energy beamforming design with channel estimation errors was discussed in [17].

Furthermore, WPT can be enhanced to support simultaneous wireless information and power transfer (SWIPT) [18], [19]. For co-located information and energy receivers, time switching and power splitting strategies were designed in [20]–[23]. If receivers are separately located, the broadcasted wireless signals can be then harvested and decoded simultaneously by different receivers. Energy beamforming can also improve the

Manuscript received February 21, 2017; revised June 26, 2017; accepted September 17, 2017. Date of publication October 6, 2017; date of current version December 8, 2017. This work was supported in part by the NSF under Grant ECCS-1554576, Grant ECCS-1610874, and Grant CNS-1320736, in part by the National Natural Science Foundation of China under Grant 61628107 and Grant 61771427, in part by the Zhejiang Provincial Public Technology Research of China under Grant 2016C31063, and in part by the Fundamental Research Funds for the Central Universities under Grant 2015XZZX001-02. The associate editor coordinating the review of this paper and approving it for publication was D. C. Popescu. (*Corresponding author: Zhao Chen.*)

Z. Chen, L. X. Cai, and Y. Cheng are with the Department of Electrical and Computer Engineering, Illinois Institute of Technology, Chicago, IL 60616 USA (e-mail: zchen84@iit.edu; lincai@iit.edu; cheng@iit.edu).

H. Shan is with the College of Information Science and Electronic Engineering, Zhejiang University, Hangzhou 310027, China (e-mail: hshan@zju.edu.cn).

Color versions of one or more of the figures in this paper are available online at <http://ieeexplore.ieee.org>.

Digital Object Identifier 10.1109/TWC.2017.2758365

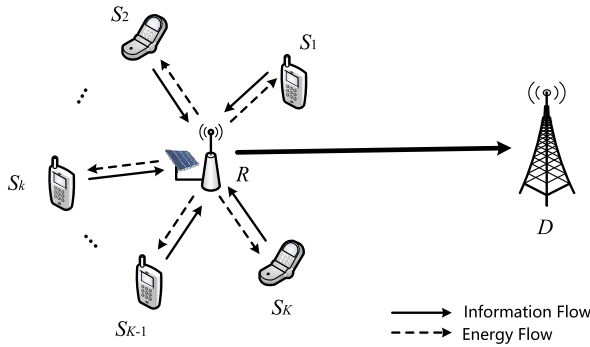


Fig. 1. A fully sustainable wireless powered cooperative communication network, which consists of K wireless powered source nodes $\{S_k\}_{k=1}^K$, one half-duplex EH relay node R and one destination node D .

efficiency of SWIPT for multi-antenna transmitters [24]–[26]. Moreover, there exists a trade-off between energy transfer and data transmission for SWIPT in multiuser networks [27], [28] and MIMO broadcasting systems [29]–[31]. Besides, opportunistic RF energy harvesting has been considered for wireless fading channels [32] and cognitive radio networks [33].

In cooperative networks, WPT has also been widely applied [34]–[40]. In [34] and [35], outage probability and system throughput have been analyzed for a classic three-node cooperative network, where the relay node works between RF charging and data decoding by time switching. Meanwhile, the power splitting strategy was investigated in [36]. In [37] and [40], the harvest-then-cooperate protocol was designed such that both the source and relay nodes are charged by the H-AP in the downlink and then work cooperatively in the uplink. More interestingly, wireless signals forwarded from the relay to the destination can be also harvested by the source node as RF energy at the same time. Such relay energy powered cooperative network has been studied for a time-slotted system in [38] and a buffer-aided system in [39], respectively.

In this paper, inspired by the technologies of EH and WPT, a fully sustainable wireless powered cooperative communication network is considered. As shown in Fig. 1, for a heterogeneous network (HetNet), the relay node is a femto-cell or pico-cell BS supplied with renewable sources, which can simultaneously transmit data bits to a destination macro BS and transfer RF energy to multiple low-power source nodes. Due to the high attenuation of wireless energy transfer over distance, the source nodes should be close to the relay node, e.g., within 20 meters. Moreover, we assume that the relay node is equipped with a data buffer and employs the buffer-aided relaying strategy as in [41] and [42], which requires each time slot to be carefully scheduled to either a source node or the relay node. Therefore, joint time scheduling and power allocation is necessary to maximize sum-throughput of the network system.

In comparison with previously studied WPT based wireless cooperative network systems [34]–[39], the proposed wireless powered cooperative network only depends on green energy at the relay node and can work sustainably without any external power supply. To the best of our knowledge, it is the first paper to investigate a fully sustainable relay energy assisted SWIPT network. Specifically, it is worth noting that in previous study

on relay energy assisted SWIPT systems [38], [39], power allocation or time scheduling is separately optimized and only a single source node is considered, while a joint time scheduling and power allocation strategy is adopted and multiple mobile users are considered to achieve better throughput performance in this work, which leads to a non-convex mixed integer nonlinear program (MINLP) with NP-hard complexity. Moreover, the formulated problem is mutually coupled with data and energy constraints between all the source nodes and the relay node, which makes it much more challenging to solve. In summary, the contributions of this paper can be briefly listed as follows:

- We propose a fully sustainable cooperative communication system model and show how to make efficient use of green energy at the relay node to forward information bits to the destination and charge multiple lower-power devices wirelessly by RF energy simultaneously. To further improve system throughput, the buffer-aided relaying strategy is also employed.
- We formulate a network throughput maximization problem to jointly optimize time scheduling and power allocation for the proposed model, which is an NP-hard non-convex MINLP problem. To obtain a tight upper bound, without directly relaxing the integer variables, we reformulate the original problem via slots reordering and combining, which can be then simplified by the DWF algorithm and iteratively solved by the sequential parametric convex approximation (SPCA) method.
- An optimal Branch-and-Bound (BnB) algorithm framework is proposed to solve the formulated offline throughput maximization problem. Moreover, the BnB method is enhanced by an efficient sub-optimal offline algorithm which can significantly reduce the time complexity from exponential to polynomial. Finally, inspired from the optimal solution to the offline problem, a heuristic online algorithm is also designed.

The rest of this paper is organized as follows. Firstly, system model and problem formulation are described in Section II. Then, an upper bound of system sum-throughput is analyzed and throughput maximization algorithms are provided in Section III and Section IV, respectively. In Section V, numerical results are presented. Finally, Section VI concludes this paper.

II. SYSTEM MODEL AND PROBLEM FORMULATION

In Fig. 1, a time division multiple access (TDMA) based wireless powered cooperative communication system is considered, which consists of K wireless powered source nodes $\{S_k\}_{k=1}^K$, one buffer-aided EH relay node R and one destination node D . It models a scenario where R is a small cell BS, D is the destination macro BS and all the source nodes are low-power mobile devices close to R . All nodes are half-duplex and equipped with single antenna. For each S_k , $k \in \mathcal{K} = \{1, \dots, K\}$, since the distance to R is much smaller than that to D , direct links are ignored and a decode-and-forward strategy is employed for the ease of implementation. Some S_k will first send information bits to R , while R can temporarily store

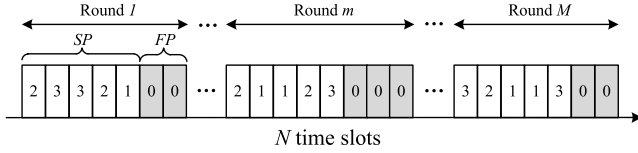


Fig. 2. Time scheduling for data transmission, where the assignment of each slot $n \in \mathcal{X}$ is indicated by the value of x_n shown in the block. Moreover, the sending phase (SP) and forwarding phase (FP) in each round are also presented. Here, we assume $K = 3$.

the received bits in a data buffer and then forward them all together to D later. To make the system fully sustainable, R is supplied with some renewable sources, while all the source nodes can be charged by the RF energy of the forwarding signals from R to transmit data in upcoming slots.¹ Therefore, the whole cooperative network system can operate sustainably without any other power supply. Note that due to the small size and low hardware cost, we assume that each S_k is only equipped with RF energy harvesters.

To maximize system throughput over a finite horizon, we assume that there are N time slots to be scheduled, where N can be considered as the delay constraint for data transmission. As of a TDMA-based network, each slot $n \in \mathcal{X} = \{1, \dots, N\}$ can be only assigned to one node. Let $x_n \in \mathcal{X} \cup \{0\}$ be an integer link indicator. As shown in Fig. 2, if $x_n = k \in \mathcal{X}$, slot n is assigned to S_k to transmit with power $p_{S_k, n}$. Otherwise for $x_n = 0$, slot n is occupied by R to forward with power $p_{R, n} + q_{R, n}$. Note that all the N time slots can be further divided into M rounds, each of which includes two phases, i.e., the sending phase for the source nodes in the beginning and the forwarding phase for the relay node in the following. Moreover, the complex channel gain between node u and v is denoted by $\tilde{h}_{u, v}$ for $u \in \mathcal{U} = \{S_1, \dots, S_K, R\}$ and $v \in \{R, D\}$. Thus, the corresponding channel power gain is represented by $h_{u, v} = |\tilde{h}_{u, v}|^2$, which is assumed perfectly known and remain constant throughout the short-term N -slot transmission in a slow-fading environment [10]–[12].

We assume that each S_k always has data bits to be transmitted. Thus, the total received bits of R up to slot n are

$$c_{S, n} = \sum_{j=1}^n \sum_{k=1}^K \mathbf{1}_{x_j=k} \cdot \log(1 + \gamma_{S_k, R} p_{S_k, j}), \quad (1)$$

where $\mathbf{1}_A$ is an indicator function of event A and $\gamma_{u, v} = h_{u, v} / \sigma_v^2$ is the normalized signal-to-noise ratio of the link from node u to v . Here, σ_v^2 is the variance of Gaussian noise. Also, the capacity of R 's data buffer is assumed to be sufficiently large to temporarily store all its received bits.

Due to data causality, the number of forwarded bits of R is limited by its buffered data bits. Since R will forward with power $p_{R, n} + q_{R, n}$,² where $p_{R, n}$ is the effective transmission power required by the rate-power function, and $q_{R, n}$ is the extra charging power to feed the source nodes with supple-

¹In the proposed system model, although it is possible for the source nodes to harvest RF energy from each other, the RF energy harvested from other source nodes is negligible compared to that harvested from the relay node.

²Although the required power is $p_{R, n}$, the relay node will modulate with power $p_{R, n} + q_{R, n}$ to transmit $\log(1 + \gamma_{R, D} p_{R, n})$ data bits. For the receiver, there is no need to separate the wireless signals into two parts.

mentary RF energy [43]. Thus, the total forwarded bits $c_{R, n}$ up to slot n can be represented by

$$c_{R, n} = \sum_{j=1}^n \mathbf{1}_{x_j=0} \cdot \log(1 + \gamma_{R, D} p_{R, j}). \quad (2)$$

From (1) and (2), the data causality constraint for R requires

$$c_{R, n} \leq c_{S, n}, \quad \forall n \in \mathcal{X}, \quad (3)$$

which indicates that the total forwarded bits should not exceed the total received bits up to any slot $n \in \mathcal{X}$. Moreover, to guarantee all the received bits at R to be entirely forwarded to D after slot N , the end-to-end system sum-throughput can be evaluated by $\min\{c_{S, N}, c_{R, N}\}$, which is the objective to be maximized in our optimization problem.

To consider energy constraints, for each node $u \in \mathcal{U}$, we denote the initial energy in its battery as $B_{u, \text{ini}}$ and the capacity of the battery as $B_{u, \text{max}}$, respectively. The per-slot duration time is normalized to be one in this paper, and thus it is equivalent to use energy and power in the context as their values will be equal. For the relay node, the energy harvested during each time slot $n \in \mathcal{X}$ is denoted by E_n , which is assumed to be non-causally known for the offline problem. Compared with the energy consumed for RF signals, we assume the energy consumption in signal processing such as decoding and re-encoding is negligible [34]–[39]. Thus, the transmission power of R at time slot n can be constrained by

$$p_{R, n} + q_{R, n} \leq b_{R, n-1}, \quad \forall n \in \mathcal{X}, \quad (4)$$

where $b_{R, n}$ denotes the residual energy of R after slot n , i.e.,

$$b_{R, n} = \min\{b_{R, n-1} + E_n - \mathbf{1}_{x_n=0} \cdot (p_{R, n} + q_{R, n}), B_{R, \text{max}}\}. \quad (5)$$

Note that $b_{R, 0} = B_{R, \text{ini}}$. Meanwhile, the transmission power of each S_k can be constrained by

$$p_{S_k, n} \leq b_{S_k, n-1}, \quad \forall n \in \mathcal{X}, \quad \forall k \in \mathcal{K}, \quad (6)$$

where $b_{S_k, n}$ denotes the residual energy of S_k after the n th slot, i.e.,

$$b_{S_k, n} = \min\{b_{S_k, n-1} + e_{S_k, n} - \mathbf{1}_{x_n=k} \cdot p_{S_k, n}, B_{S_k, \text{max}}\}. \quad (7)$$

Note that $b_{S_k, 0} = B_{S_k, \text{ini}}$ and $e_{S_k, n}$ is defined as the RF energy charged from R during slot n ,

$$e_{S_k, n} = \mathbf{1}_{x_n=0} \cdot \phi_{R, S_k} (p_{R, n} + q_{R, n}), \quad (8)$$

where $\phi_{R, S_k} = \eta h_{S_k, R}$ is the power transfer efficiency from R to S_k and $\eta \in (0, 1)$ is the energy conversion efficiency factor. Here, we also assume channel reciprocity holds for each downlink and uplink of S_k .

In order to guarantee sustainability of the network, each node $u \in \mathcal{U}$ also requires a minimum residual energy of $B_{u, \text{res}}$ after slot N , which can be represented by

$$b_{u, N} \geq B_{u, \text{res}}, \quad \forall u \in \mathcal{U}. \quad (9)$$

Therefore, to maximize the system sum-throughput, we need to jointly optimize time scheduling over x_n and power allocation over p_{S_k} , $p_{R,n}$ and $q_{R,n}$, which gives the following

$$(P1) : \max_{x_n, p_{S_k, n}, p_{R, n}, q_{R, n}} \min\{c_{S, N}, c_{R, N}\} \quad (10)$$

$$\text{s.t. (3), (4), (6) and (9),}$$

$$p_{S_k, n}, p_{R, n}, q_{R, n} \geq 0, \quad x_n \in \mathcal{X} \cup \{0\}, \quad \forall n, \quad \forall k. \quad (11)$$

Remark 1: (P1) is a non-convex MINLP problem due to the integer indicators x_n and the non-convex and non-linear constraints, which is NP-hard and difficult to solve. Besides, the objective (10) can be simplified by $c_{R, N} = \min\{c_{S, N}, c_{R, N}\}$, since the condition in (3) gives $c_{R, N} \leq c_{S, N}$. Later, we will analyze the upper bound of (P1) by relaxation and then solve it with optimal and sub-optimal algorithms, respectively.

III. UPPER BOUND ANALYSIS

In this section, we will analyze the upper bound of (P1) by reformulation and relaxation, which can estimate the system performance and inspire us to design heuristic algorithms.

A. Problem Reformulation

Rather than directly relaxing integers x_n to be continuous, we reformulate each round in (P1) by introducing *epochs*. That is, during the sending phase of each round $m \in \mathcal{M} = \{1, \dots, M\}$, all the time slots assigned to the same source node S_k can be reordered together and combined as an epoch k as shown in Fig. 3, whose length is denoted by $n_{S_k, m}$. The following lemma shows the property of epochs.

Lemma 1: All the time slots assigned to S_k in round $m \in \mathcal{M}$ can be reordered together as the k th epoch without decreasing the throughput performance. Moreover, the optimal transmission power of S_k remains constant during the epoch.

Proof: Due to the constant channel power gain $h_{S_k, R}$, reordering of the assigned slots for each S_k will not affect the total throughput, if the transmission power of each slot keeps unchanged. Hence, the total energy consumption of each S_k is fixed and the energy constraints will still hold after reordering, since each S_k will not be charged during the sending phase. In this way, given the amount of energy consumption and the number of assigned slots for each S_k , a constant transmission power will achieve higher throughput than any other strategies owing to the concavity of the rate-power function. \square

Although time slots assigned to R in the forwarding phase can be combined as epoch 0 of length $n_{R, m}$, the property of constant transmission power does not hold due to the random energy arrivals during the epoch. Nevertheless, it can be shown later such property holds for R after problem relaxation.

B. Problem Relaxation

After reformulation, the upper bound of (P1) can be derived by relaxing the discrete epoch lengths $n_{S_k, m}$ and $n_{R, m}$ to be continuous for all $m \in \mathcal{M}$, which are denoted by $\tau_{S_k, m}$ and $\tau_{R, m}$, respectively. In this case, the total transmission time can

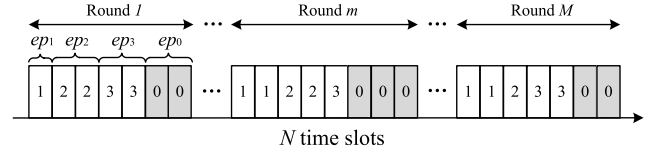


Fig. 3. Problem reformulation for the example in Fig. 2, where in each round, time slots assigned to the source nodes are reordered and combined into K epochs as $ep_1 \sim ep_K$ and the epoch for the relay node is denoted as ep_0 .

be written by $T = N$, and the number of rounds M is assumed to be a sufficiently large integer. Thus, the total received bits of R after round m can be represented by

$$\bar{c}_{S, m} = \sum_{j=1}^m \sum_{k=1}^K \tau_{S_k, j} \log(1 + \gamma_{S_k, R} \bar{p}_{S_k, j}), \quad (12)$$

where $\bar{p}_{S_k, m}$ is the transmission power of S_k during epoch k of round m .

Meanwhile, the forwarding power of R can be written by $\bar{p}_{R, m} + \bar{q}_{R, m}$, where $\bar{p}_{R, m}$ and $\bar{q}_{R, m}$ are constant effective transmission and extra charging powers during the forwarding phase, respectively. If the $\bar{p}_{R, m}$ or $\bar{q}_{R, m}$ changes during the forwarding phase, such round m can be always divided into two rounds to guarantee constant powers in each round. Hence, the total forwarded bits of R can be written by

$$\bar{c}_{R, m} = \sum_{j=1}^m \tau_{R, j} \log(1 + \gamma_{R, D} \bar{p}_{R, j}). \quad (13)$$

By relaxation, the capacity of each node u 's battery is assumed to be sufficiently large, i.e., $B_{u, \max} = +\infty$ for $\forall u \in \mathcal{U}$. Thus, given $B_{R, \text{ini}}$, the green energy that can be consumed by R up to time t is $B_{R, \text{ini}} + \sum_{j=1}^{\lceil t \rceil - 1} E_j$,³ since the most recent energy arrives at slot $n = \lceil t \rceil - 1$. Moreover, due to the residual energy requirement, the total consumed energy of R after time T cannot exceed $B_{R, \text{ini}} + \sum_{j=1}^N E_j - B_{R, \text{res}}$. Therefore, we can define the *total available energy* of R up to any time $t \in (0, T]$ as follows,

$$f_E(t) = B_{R, \text{ini}} + \min \left\{ \sum_{j=1}^{\lceil t \rceil - 1} E_j, \sum_{j=1}^N E_j - B_{R, \text{res}} \right\}, \quad (14)$$

Additionally, we define $f_E(0) = 0$. As a result, $f_E(t)$ gives the upper bound of total energy that can be consumed by R up to time $t \in [0, T]$, which gives the solid curve in Fig. 4.

By (14), the forwarding power of R will be constrained by

$$\sum_{j=1}^m \tau_{R, j} (\bar{p}_{R, j} + \bar{q}_{R, j}) \leq f_E \left(\sum_{j=1}^m \left(\sum_{k=1}^K \tau_{S_k, j} + \tau_{R, j} \right) \right), \quad \forall m \in \mathcal{M}, \quad (15)$$

which follows from (4) and ensures the total consumed energy of R does not exceed its total available energy up to round m . Meanwhile, given $B_{S_k, \text{ini}}$ and according to (6), the transmission power of S_k in each round m is constrained by

$$\sum_{j=1}^m \tau_{S_k, j} \bar{p}_{S_k, j} \leq B_{S_k, \text{ini}} + \sum_{j=1}^{m-1} \phi_{R, S_k} \tau_{R, j} (\bar{p}_{R, j} + \bar{q}_{R, j}), \quad \forall k \in \mathcal{K}, \quad \forall m \in \mathcal{M}. \quad (16)$$

³Note that $\lceil x \rceil$ denotes the smallest integer greater than or equal to x .

What is more, considering the residual energy constraint in (9), the total consumed energy of each S_k will be constrained by

$$\sum_{j=1}^M \tau_{S_k,j} \bar{p}_{S_k,j} \leq B_{S_k,\text{ini}} + \sum_{j=1}^M \phi_{R,S_k} \tau_{R,j} (\bar{p}_{R,j} + \bar{q}_{R,j}) - B_{S_k,\text{res}}, \quad \forall k \in \mathcal{K}. \quad (17)$$

Therefore, the relaxed problem of (P1) is formulated as,

$$(P2) : \quad \max_{\tau_{S_k,m}, \tau_{R,m}, \bar{p}_{S_k,m}, \bar{p}_{R,m}, \bar{q}_{R,m}} \bar{c}_{R,M} \\ \text{s.t. } \bar{c}_{R,m} \leq \bar{c}_{S,m}, \quad \forall m \in \mathcal{M}, \quad (18) \\ (15), (16) \text{ and } (17),$$

$$\sum_{j=1}^M \left(\sum_{k=1}^K \tau_{S_k,j} + \tau_{R,j} \right) \leq T, \quad (19)$$

where the constraints in (18) guarantee the data causality and the constraint in (19) is due to the total transmission time T . It is worth noting that (P2) is not convex due to the constraints in (18). Besides, the source nodes' energy dependency on the relay node in (16) makes it more difficult to be handled.

C. Optimal Solution to the Relaxed Problem

In order to solve problem (P2), which is also referred to as the general model, a fixed energy model that simplifies (P2) by replacing all the random energy arrivals at R with an aggregate initial energy is considered. Later, the fixed energy model will be employed as sub-problems to solve the general model.

1) *Fixed Energy Model*: Assume all the energy that can be consumed by R during the whole transmission time T is initially given as a fixed amount E_R . Thus, there will be no more energy arrivals and we only need to check the total energy consumption of R after time T , which indicates that the constraints in (15) can be replaced by

$$\sum_{m=1}^M \tau_{R,m} (\bar{p}_{R,m} + \bar{q}_{R,m}) \leq E_R. \quad (20)$$

To be more general, we also assume the number of initial and residual information bits in R 's data buffer to be d_{ini} and d_{res} , respectively. In this case, the data causality constraints in (18) can be modified by

$$\bar{c}_{R,m} \leq d_{\text{ini}} + \bar{c}_{S,m} - \mathbf{1}_{m=M} \cdot d_{\text{res}}, \quad \forall m \in \mathcal{M}. \quad (21)$$

With (20) and (21), the fixed energy model can be formulated as the following (P3),

$$(P3) : \quad \max_{\tau_{S_k,m}, \tau_{R,m}, \bar{p}_{S_k,m}, \bar{p}_{R,m}, \bar{q}_{R,m}} \bar{c}_{R,M} \\ \text{s.t. } (16), (17), (19), (20) \text{ and } (21).$$

Remark 2: (P3) reveals some properties of the optimal solution to (P2), since it still considers the energy dependency of the source nodes on the relay node. If the total transmission time T , the parameters of R , i.e., E_R , d_{ini} and d_{res} , and the parameters of each S_k , i.e., $B_{S_k,\text{ini}}$ and $B_{S_k,\text{res}}$, are given, the optimal solution to (P3) is determined. Here, (P3) is still not a convex optimization problem due to the constraints in (21).

To tackle (P3), it can be further relaxed by removing each S_k 's energy dependency on R . In this way, similar to (20), each S_k could non-causally expend the RF energy from R , i.e., each S_k is now constrained by a pre-harvested total energy E_{S_k} and the constraints of (16) and (17) can be replaced by

$$\sum_{m=1}^M \tau_{S_k,m} \bar{p}_{S_k,m} \leq E_{S_k} = B_{S_k,\text{ini}} + \phi_{R,S_k} E_R - B_{S_k,\text{res}}, \quad (22)$$

for $\forall k \in \mathcal{K}$. Therefore, it can be regarded as a sum-throughput maximization problem for a buffer-aided relaying system with an independent energy constraint for each node and a total shared time T . Hence, all the epochs for each node $u \in \mathcal{U}$ can be combined into an accumulated epoch $T_u = \sum_{j=m}^M \tau_{u,m}$, and eventually there will be only one round, i.e., $M = 1$. Also, it is worth noting that all the energy of R will be used to transmit data bits and the extra charging power will be $\bar{q}_{R,m} = 0$ for each $m \in \mathcal{M}$. In summary, we have the following problem (P4),

$$(P4) : \quad \max_{T_{S_k}, T_R} \min \left\{ T_R \log \left(1 + \frac{\gamma_{R,D} E_R}{T_R} \right), \right. \\ \left. \sum_{k=1}^K T_{S_k} + T_R \leq T \right. \\ \left. d_{\text{ini}} + \sum_{k=1}^K T_{S_k} \log \left(1 + \frac{\gamma_{S_k,R} E_{S_k}}{T_{S_k}} \right) - d_{\text{res}} \right\}. \quad (23)$$

Fortunately, (P4) is a convex problem⁴ [44], whose optimal solution can be given in the following theorem.

Theorem 1: For (P4), the optimal value T_R^* is given by the root of the following equation:

$$T_R \log \left(1 + \frac{\gamma_{R,D} E_R}{T_R} \right) \\ = d_{\text{ini}} + (T - T_R) \log \left(1 + \frac{\sum_{k=1}^K \gamma_{S_k,R} E_{S_k}}{T - T_R} \right) - d_{\text{res}}, \quad (24)$$

and then the optimal value $T_{S_k}^* = \frac{\gamma_{S_k,R} E_{S_k} (T - T_R^*)}{\sum_{j=1}^K \gamma_{S_j,R} E_{S_j}}$.

Proof: Please refer to Appendix A. \square

With Theorem 1, the optimal transmission power of each S_k can be written by $P_{S_k}^* = \frac{E_{S_k}}{T_{S_k}^*} = \frac{\sum_{j=1}^K \gamma_{S_j,R} E_{S_j}}{\gamma_{S_k,R} (T - T_R^*)}$ and the optimal effective power of R can be obtained by $P_R^* = \frac{E_R}{T_R^*}$. Moreover, it is worth noting that if $\gamma_{R,D} E_R \gg \sum_{k=1}^K \gamma_{S_k,R} E_{S_k}$, (24) can be approximated by

$$T_R^* \log \left(1 + \frac{\gamma_{R,D} E_R}{T_R^*} \right) \\ \approx C_{\text{UP}} = d_{\text{ini}} + T \log \left(1 + \frac{\sum_{k=1}^K \gamma_{S_k,R} E_{S_k}}{T} \right) - d_{\text{res}}, \quad (25)$$

from which we can obtain

$$T_R^* \approx \frac{C_{\text{UP}}}{-\mathcal{W} \left(-\frac{C_{\text{UP}}}{\gamma_{R,D} E_R} e^{-\frac{C_{\text{UP}}}{\gamma_{R,D} E_R}} \right) - \frac{C_{\text{UP}}}{\gamma_{R,D} E_R}}. \quad (26)$$

Note that function $\mathcal{W}(z)$ is the Lambert W function [45] which satisfies $\mathcal{W}(z) e^{\mathcal{W}(z)} = z$.

⁴The objective of (P4) is concave because the perspective of a concave function and the pointwise minimum of concave functions preserve concavity.

The optimal solution to (P4) can be extended to solve (P3) in the following theorem, which reveals that the same sum-throughput of (P4) can be achieved by (P3) by satisfying the energy dependency constraints of source nodes in (16).

Algorithm 1 OptSchedule($\{T_{S_k}\}, \{P_{S_k}\}, T_R, P_R, \{B_{S_k,0}\}$)

- 1: Set initial energy: $\bar{b}_{S_k} = B_{S_k,0}$ and $\bar{b}_R = E_R = P_R T_R$;
 - 2: Set time ratio for each S_k to R : $\alpha_{S_k,R} = \frac{T_{S_k}}{T_R}$;
 - 3: Set round index: $m = 1$;
 - 4: **while** $\bar{b}_R > 0$ **do**
 - 5: $\tau_{R,m} = \min \left\{ \frac{\bar{b}_R}{P_R}, \min_{1 \leq k \leq K} \left\{ \frac{1}{\alpha_{S_k,R}} \cdot \frac{\bar{b}_{S_k}}{P_{S_k}} \right\} \right\}$;
 - 6: **for each** $k = 1 : K$ **do**
 - 7: $\tau_{S_k,m} = \alpha_{S_k,R} \cdot \tau_{R,m}$;
 - 8: $\bar{b}_{S_k} = \bar{b}_{S_k} - \tau_{S_k,m} P_{S_k} + \phi_{R,S_k} \tau_{R,m} P_R$;
 - 9: **end for**
 - 10: $\bar{b}_R = \bar{b}_R - \tau_{R,m} P_R$, $m = m + 1$;
 - 11: **end while**
 - 12: $M = m$;
 - 13: Return the number of rounds M and all scheduled epochs $\{\{\tau_{S_k,m}\}_{k=1}^K\}_{m=1}^M$ and $\{\tau_{R,m}\}_{m=1}^M$.
-

Theorem 2: For (P3), there exists an optimal solution such that for each round $m \in \mathcal{M}$, the optimal powers of each source node S_k and the relay node R remain constant as $\bar{p}_{S_k,m}^* = P_{S_k}^*$ and $\bar{p}_{R,m}^* = P_R^*$. Moreover, the total number of rounds and the optimally scheduled epochs can be obtained by calling OptSchedule($\{T_{S_k}^*\}, \{P_{S_k}^*\}, T_R^*, P_R^*, \{B_{S_k,ini}\}$) in Algorithm 1.

Proof: In Algorithm 1, it is guaranteed that for each round m , the consumed energy of each node $u \in \mathcal{U}$ in the network will not exceed its current battery storage \bar{b}_u in Line 5 and the total number of received and forwarded bits of R equals in Line 8. The transmission will continue until the available energy of R , i.e., \bar{b}_R , depletes. Therefore, with the same optimal transmission power and accumulated epoch time for each node, the maximum sum-throughput achieved by Algorithm 1 for (P3) is equal to that of (P4). Considering that the optimal value of (P3) is upper bounded by (P4), we have obtained the optimal solution to (P3). \square

Remark 3: For any feasible solution to the general model, we can define the *average power* of each round $m \in \mathcal{M}$ for R as $p_{R,m}^{\text{avg}} = \frac{\bar{p}_{R,m} \tau_{R,m}}{\sum_{k=1}^K \tau_{S_k,m} + \tau_{R,m}}$. From Theorem 2, it can be verified that in the fixed energy model, the optimal average power $p_{R,m}^{\text{avg}*}$ for each round m remains constant as

$$p_{R,m}^{\text{avg}*} = p_{R,1}^{\text{avg}*} = \dots = p_{R,m}^{\text{avg}*} = \dots = p_{R,M}^{\text{avg}*} = \frac{E_R}{T}, \quad (27)$$

which is only decided by the fixed energy of the relay node E_R and the total transmission time T , unlike the optimal effective transmission power $\bar{p}_{R,m}^* = P_R^*$ that will be affected by other parameters, i.e., the initial and residual state of each node's battery and the relay's data buffer. Such property is important to derive the optimal solution to the general model.

2) *General Model:* Now we employ the fixed energy model to solve the general model, i.e., the relax problem (P2), by considering the random energy arrivals again. In prior works on

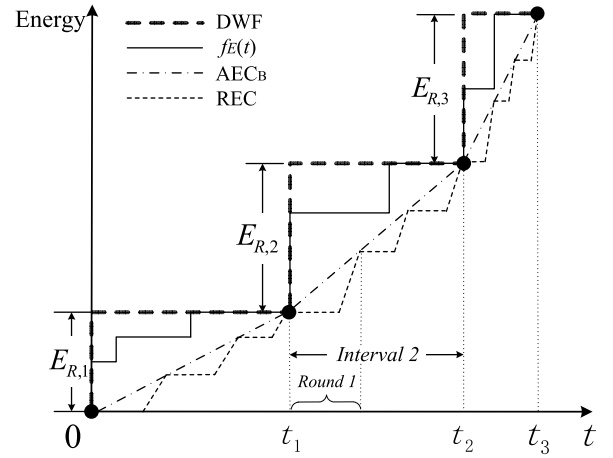


Fig. 4. Illustration of accumulative energy curves at the relay node, including the energy constraining curves $f_E(t)$ and DWF, and the energy consumption curves AEC_B and REC. Here, we assume $I = 3$ for the $f_E(t)$ curve.

point-to-point EH enabled communication systems [7]–[9], the DWF algorithm has been proposed to solve offline throughput maximization problems with optimal power allocation. Due to the concavity of rate-power function, the obtained optimal powers are non-decreasing and will remain constant as long as possible until the current available energy of the transmission node is exhausted. Moreover, the optimal powers only potentially change when new energy arrives. If we define such power changing points in the DWF algorithm as *DWF points* and assume that there are I DWF points for the $f_E(t)$ curve, each DWF point $(t_i, \sum_{j=1}^i E_{R,i})$ can be derived by

$$t_i = \arg \min_{t \leq T, t > t_{i-1}} \left\{ \frac{f_E(t) - f_E(t_{i-1})}{t - t_{i-1}} \right\}, \quad (28)$$

$$E_{R,i} = f_E(t_i) - f_E(t_{i-1}), \quad (29)$$

for each $i \in I = \{1, 2, \dots, I\}$, where we define $t_0 = 0$ and $t_I = T$. Consequently, $f_E(t)$ is reorganized into I intervals, each of which has a duration $T_i = t_i - t_{i-1}$. We also define a *DWF energy profile* $\{E_{R,i}\}_{i=1}^I$ for all intervals. Recall that the total transmission time T is divided into M rounds. Now, we assume each interval $i \in I$ contains M_i rounds and each round belongs to only one interval, as illustrated in Fig. 4. If one round covers two intervals, it can be further separated into two rounds that belong to different intervals respectively.

To describe the accumulative energy consumption of R , the *real energy consumption* (REC) curve and the *average energy consumption* (AEC) curve can be defined as shown in Fig. 4. The REC curve records the amount of energy consumed up to time t , where for each round, e.g., round 1 in interval 2, it can be seen that the flat part is the sending phase followed by the rising part, i.e., the forwarding phase. Note that the REC curve should be on the right side of $f_E(t)$, otherwise the energy constraints is violated. As for the AEC curve, it is obtained by connecting the starting point and ending point of each round in the obtained solution, whose slope represents the average power of the corresponding round. For the fixed energy model, we have remarked the constant average power property of R in (27) according to Theorem 2. As for the general model with random energy

arrivals, the following lemma investigates the property of the average power in (P2)'s optimal solution.

Lemma 2: The average power of the relay node R for each round is non-decreasing in the optimal solution to (P2).

Proof: Please refer to Appendix B. \square

It can be inferred from Lemma 2 that the slope of the AEC curve of the optimal solution is non-decreasing. Then, if we define the AEC_B curve by connecting all the DWF points sequentially from the origin point as shown in Fig. 4, it can be proved to be the upper bound for the optimal AEC curve.

Lemma 3: The AEC curve of the optimal solution to (P2) is upper bounded by the AEC_B curve.

Proof: Please refer to Appendix C. \square

As the optimal AEC curve is upper bounded by the AEC_B curve, the optimal solution can be obtained by replacing the random energy profile $\{E_n\}_{n=1}^N$ and employing the DWF energy profile $\{E_{R,i}\}_{i=1}^I$ non-causally. That is, for each interval $i \in I$, it is equivalent to assume that there would be an energy arrival $E_{R,i}$ available at the beginning of that interval. The two different energy profiles will give the same optimal AEC curve. Thus, with the non-causal DWF energy profile, (P2) can be reduced and solved by I sub-problems.

Lemma 4: If the $f_E(t)$ curve is reorganized into I intervals by the DWF algorithm, (P2) can be decomposed into I sub-problems, each of which can be solved as an instance of (P3).

Proof: Given any feasible solution of (P2), for each interval $i \in I$, we can calculate the total consumed energy of R as the fixed energy E_R in (P3), and record the initial and residual states of each source node's battery and the relay node's data buffer, which can be then configured as input parameters for (P3). Thus, the optimal solution for interval i can be given by Theorem 2 without affecting any state of other intervals. Besides, the average power of the relay node will be constant for each round in the i th interval, which indicates that the energy constraints still hold for the newly obtained solution. Therefore, the optimal solution to (P2) can be obtained by solving I sub-problems for all the intervals. \square

Although (P2) can be decomposed into I sub-problems by (P3), the consumed energy and accumulated epoch of each node $u \in \mathcal{U}$ during each interval $i \in I$, i.e., $\Theta_{u,i}$ and $T_{u,i}$, still need to be optimized. By Lemma 3, $\Theta_{R,i}$ can be equivalently bounded by the non-causal DWF energy profile. Meanwhile, similar to the relaxation of (P3) using (22), for each S_k , $\Theta_{S_k,i}$ is also bounded by the non-causal RF energy charged from R. Thus, for each $i \in I$ and $k \in \mathcal{K}$, we have an equivalent sum-throughput maximization problem of (P2) as follows,

$$(P5) : \max_{T_{S_k,i}, T_{R,i}, \Theta_{S_k,i}, \Theta_{R,i}} \sum_{i=1}^I T_{R,i} \log\left(1 + \frac{\gamma_{R,D} \Theta_{R,i}}{T_{R,i}}\right) \quad (30)$$

$$\text{s.t. } \sum_{j=1}^i T_{R,j} \log\left(1 + \frac{\gamma_{R,D} \Theta_{R,j}}{T_{R,j}}\right) \\ \leq \sum_{j=1}^i \sum_{k=1}^K T_{S_k,j} \log\left(1 + \frac{\gamma_{S_k,R} \Theta_{S_k,j}}{T_{S_k,j}}\right), \quad \forall i, \quad (31)$$

$$\sum_{j=1}^i \Theta_{R,i} \leq \sum_{j=1}^i E_{R,j}, \quad \forall i, \quad (32)$$

$$\sum_{j=1}^i \Theta_{S_k,i} \leq B_{S_k,\text{ini}} + \phi_{R,S_k} \sum_{j=1}^i \Theta_{R,j} \\ - \mathbf{1}_{i=L} \cdot B_{S_k,\text{res}}, \quad \forall i, \quad \forall k, \quad (33)$$

$$\sum_{k=1}^K T_{S_k,i} + T_{R,i} \leq T_i, \quad \forall i, \quad (34)$$

where the constraints in (31) follow from the data causality constraints, the constraints in (32) is owing to the equivalent non-causal DWF energy profile, the constraints in (33) are due to the non-causal RF energy dependency of the source nodes on the relay node, and the constraints in (34) follow from the duration of each interval. (P5) is still a non-convex optimization problem due to the constraints in (31). Then, the sequential parametric convex approximation (SPCA) method [46] can be applied to linearize these non-convex constraints, which will be illustrated in Section IV by solving (P6) in a more generalized form of (P5).

With the obtained optimal consumed energy $\Theta_{u,i}^*$ and accumulated epoch $T_{u,i}^*$ of each node $u \in \mathcal{U}$ for each interval $i \in I$, we can further derive the optimal solution to (P2) by considering the energy dependency inside each interval.

Algorithm 2 Joint Time Scheduling and Power Allocation

- 1: Solve (P5) to obtain optimal values $\{\{\Theta_{S_k,i}^*\}_{k=1}^K\}_{i=1}^I$, $\{\{\Theta_{R,i}^*\}_{i=1}^I\}$, $\{\{T_{S_k,i}^*\}_{k=1}^K\}_{i=1}^I$, $\{T_{R,i}^*\}_{i=1}^I$;
 - 2: Set the initial energy of each source node: $\beta_{S_k} = B_{S_k,\text{ini}}$;
 - 3: **for** each interval $i = 1 : I$ **do**
 - 4: Obtain the optimal powers for all rounds: $P_{R,i}^* = \frac{\Theta_{R,i}^*}{T_{R,i}^*}$ and $P_{S_k,i}^* = \frac{\Theta_{S_k,i}^*}{T_{S_k,i}^*}$ for $k \in \mathcal{K}$;
 - 5: Obtain the number of rounds M_i and all optimally scheduled epochs $\{\{\tau_{S_k,m,i}\}_{k=1}^K\}_{m=1}^{M_i}$ and $\{\tau_{R,m,i}\}_{m=1}^{M_i}$ by OptSchedule($\{T_{S_k,i}^*\}$, $\{P_{S_k,i}^*\}$, $T_{R,i}^*$, $P_{R,i}^*$, $\{\beta_{S_k}\}$) in Algorithm 1;
 - 6: Update $\beta_{S_k} = \beta_{S_k} + \phi_{R,S_k} \Theta_{R,i}^* - \Theta_{S_k,i}^*$ for $k \in \mathcal{K}$;
 - 7: **end for**
 - 8: Return the number of rounds $\{M_i\}_{i=1}^I$, the optimal powers $\{\{P_{S_k,i}^*\}_{k=1}^K\}_{i=1}^I$ and $\{P_{R,i}^*\}_{i=1}^I$, and scheduled epochs $\{\{\tau_{S_k,m,i}\}_{k=1}^K\}_{m=1}^{M_i}\}_{i=1}^I$ and $\{\{\tau_{R,m,i}\}_{m=1}^{M_i}\}_{i=1}^I$.
-

Lemma 5: For (P2), there exists an optimal solution such that for each interval $i \in I$, the optimal consumed energy $\Theta_{u,i}^$ and accumulated epoch $T_{u,i}^*$ of each node $u \in \mathcal{U}$ are given by (P5). Moreover, inside interval i , the optimal power of each node u remains constant as $P_{u,i}^* = \frac{\Theta_{u,i}^*}{T_{u,i}^*}$ for all rounds, and the optimal time scheduling can be obtained by Algorithm 2.*

Proof: On one hand, by Lemma 4, we know that the optimal solution to (P2) contains the results for the I intervals. For each interval $i \in I$, we can record the optimal consumed energy $\Theta_{u,i}^{\text{opt}}$ and accumulated epoch $T_{u,i}^{\text{opt}}$ of each node $u \in \mathcal{U}$. Since such optimal values are a feasible solution to (P5), it indicates that the maximum of (P2) is upper bounded by that of (P5).

On the other hand, as described in Algorithm 2, by solving (P5), we can first obtain the optimal consumed energy $\Theta_{u,i}^*$ and accumulated epoch $T_{u,i}^*$ of each node $u \in \mathcal{U}$ for each

interval $i \in I$, respectively. Then, the optimal powers of each node during each interval can be calculated in Line 4. Finally, to address the energy dependency of the source nodes on the relay node inside each interval, the number of rounds and optimally scheduled epochs can be found using Algorithm 1 as in Line 5. Notice that the optimal solution given by Algorithm 2 is a feasible solution of (P2), because it satisfies all the constraints of (P2). Thus, the maximum of (P5) is also upper bounded by that of (P2). Therefore, we know that the maximum of (P2) is equal to that of (P5), and the optimal solution to (P2) can be obtained by Algorithm 2. \square

IV. THROUGHPUT MAXIMIZATION ALGORITHMS

A. Optimal BnB Framework

For non-convex MINLP problems, globally optimal solution can be given by the BnB optimization method [47], which will partition the original solution space of (P1) into subsets with different sub-problems and solve these sub-problems of (P1) sequentially. If \mathcal{P} denotes the sub-problem set of (P1), each sub-problem $p \in \mathcal{P}$ is defined as a branch and its upper and lower bounds, i.e., $u(p)$ and $l(p)$, can be evaluated by problem relaxation and some heuristic algorithms of (P1), respectively. If the upper bound of a branch $u(p)$ is lower than the current feasible lower bound L , it will be pruned. Hence, the tightness of bound estimation dominates the performance of the BnB framework. Assuming $p(\mathbf{x}_n)$ denotes a sub-problem of (P1) with the first n integer link indicators $\mathbf{x}_n = (x_j)_{j=1}^n$ being assigned, we describe the BnB framework in Algorithm 3.

For any sub-problem $p \in \mathcal{P}$, we denote \mathbf{x}_{N_0} to be the vector of its assigned N_0 link integer indicators. To obtain the upper bound of p , it can be estimated by the same relaxation technique in Section III-B for the last $N - N_0$ unassigned time slots, while only power allocation is needed for the first N_0 assigned slots. The initial energy for the last $N - N_0$ slots of the relay node, i.e., b_{R,N_0} , is also the residual energy after the first N_0 slots, which is now a variable determined by the power allocation of the first N_0 slots. Thus, the DWF energy profile $\{E_{R,i}\}_{i=1}^I$ and interval durations $\{T_i\}_{i=1}^I$ for the last $N - N_0$ time slots can be obtained by,

$$t_i = \arg \min_{t \leq T, t > t_{i-1}} \left\{ \frac{\sum_{j=\lceil t_{i-1} \rceil}^{\lceil t_i \rceil - 1} E_j}{t - t_{i-1}} \right\}, \quad E_{R,i} = \sum_{j=\lceil t_{i-1} \rceil}^{\lceil t_i \rceil - 1} E_j, \quad (35)$$

where we define $t_0 = N_0$, $t_I = T$ and $T_i = t_i - t_{i-1}$. Thus, for each $n \in \mathcal{N}_0 = \{1, \dots, N_0\}$, $i \in I$ and $k \in \mathcal{X}$, the upper bound of sub-problem p can be estimated by (P6) in (36)-(42), as shown at the top of the next page, where the constraints in (37) and (38) hold because of data causality, and the constraints in (39)-(41) are due to energy causality. It is worth noting that if $N_0 = 0$, (P6) will be reduced to (P5). By solving (P6), the optimal power allocation for the N_0 assigned slots can be obtained. As for the last $N - N_0$ unassigned time slots, with the optimal values of $\Theta_{S_k,i}^*$, $\Theta_{R,i}^*$, $T_{S_k,i}^*$, $T_{R,i}^*$ for the I intervals, the optimal time scheduling and power allocation can be derived by the same technique employing Algorithm 2.

Algorithm 3 The BnB Framework for (P1)

```

1: Set the sub-problem set  $\mathcal{P} = \{p_0\}$ ,  $p_0$  is the original (P1);
2: Set the upper bound  $U = u(p_0)$ , and the current feasible
   lower bound  $L = -\infty$ ;
3: while  $\mathcal{P} \neq \emptyset$  do
4:   Set sub-problem  $p = \arg \max_{p \in \mathcal{P}} u(p)$  and  $U = u(p)$ ;
5:   if  $l(p) > L$  then
6:      $L = l(p)$ ;
7:     if  $L > (1 - \epsilon)U$  then
8:       Return the  $(1 - \epsilon)$ -optimal solution  $L$ ;
9:     else
10:      Remove all  $p' \in \mathcal{P}$  satisfies  $(1 - \epsilon)u(p') < L$ ;
11:    end if
12:  end if
13:  Let  $\mathbf{x}_n$  be the  $n$  assigned link indicators of  $p$ ;
14:  for each  $x \in \mathcal{X} \cup \{0\}$  do
15:    Construct sub-problem  $p(\mathbf{x}_{n+1})$  for  $\mathbf{x}_{n+1} = (\mathbf{x}_n, x)$ ;
16:    if  $(1 - \epsilon)u(p(\mathbf{x}_{n+1})) > L$  then
17:       $\mathcal{P} = \mathcal{P} \cup \{p(\mathbf{x}_{n+1})\}$ ;
18:    end if
19:  end for
20: end while
21: Return the  $(1 - \epsilon)$ -optimal solution  $L$ .

```

Algorithm 4 Solving (P6) With the SPCA Method

```

1: Set  $b = 0$ ,  $C = -\infty$ ,  $C^{(0)} = 0$ ;
2: Set  $\mathbf{p}_{R,n}^{(0)}$ ,  $\mathbf{T}_{R,i}^{(0)}$  and  $\Theta_{R,i}^{(0)}$  to be a small positive value;
3: while  $|C - C^{(b)}| > \epsilon$  do
4:    $C = C^{(b)}$ ,  $b = b + 1$ ;
5:   Update the corresponding LHS of all the
     constraints in (37) and (38) by  $f_n^{(b)}(\mathbf{p}_{R,n})$  and
      $g_i^{(b)}(\mathbf{p}_{R,N_0}, \mathbf{T}_{R,i}, \Theta_{R,i})$ , respectively; Solve the
     updated (P6) and obtain the maximum value  $C^{(b)}$ 
     and solutions  $\mathbf{p}_{R,N_0}^{(b)}$ ,  $\mathbf{T}_{R,i}^{(b)}$ , and  $\Theta_{R,i}^{(b)}$ ;
6: end while
7: Return  $C^{(b)}$  and  $\mathbf{p}_{R,N_0}^{(b)}$ ,  $\mathbf{T}_{R,i}^{(b)}$ , and  $\Theta_{R,i}^{(b)}$ .

```

Since (P6) is non-convex due to the constraints in (37) and (38), we will linearize these non-convex constraints using the SPCA method [46], which iteratively approximates the non-convex constraint with linear ones until it converges. For instance, $c_{R,n}$ in (37) is a concave function of the variables $\mathbf{p}_{R,n} = (p_{R,j})_{j=1}^n$. The SPCA method will replace $c_{R,n}$ by its linear upper approximation $f_n^{(b)}(\mathbf{p}_{R,n})$ in the b -th iteration for a positive index b . The linear approximation $f_n^{(b)}(\mathbf{p}_{R,n})$ is constructed to be tangent to the curve of the non-convex constraint at the point $\mathbf{p}_{R,n}^{(b-1)}$,

$$f_n^{(b)}(\mathbf{p}_{R,n}) = \sum_{j=1}^n \frac{\mathbf{1}_{x_j=0} \cdot \gamma_{R,D}}{1 + \gamma_{R,D} p_{R,j}^{(b-1)}} (p_{R,j} - p_{R,j}^{(b-1)}) + c_{R,n}^{(b-1)}. \quad (45)$$

Note that $c_{R,n}^{(b-1)}$ and $\mathbf{p}_{R,n}^{(b-1)}$ are the optimal values of $c_{R,n}$ and $\mathbf{p}_{R,n}$ after the $(b-1)$ -th iteration, respectively. Similarly, the LHS of constraints in (38) can be linearly upper approx-

$$(P6) : \max_{\substack{p_{S_k,n}, p_{R,n}, q_{R,n}, \\ T_{S_k,i}, T_{R,i}, \Theta_{S_k,i}, \Theta_{R,i}}} c_{R,N_0} + \sum_{i=1}^I T_{R,i} \log\left(1 + \frac{\gamma_{R,D} \Theta_{R,i}}{T_{R,i}}\right) \quad (36)$$

$$\text{s.t. } c_{R,n} \leq c_{S,n}, \quad \forall n, \quad (37)$$

$$c_{R,N_0} + \sum_{j=1}^i T_{R,j} \log\left(1 + \frac{\gamma_{R,D} \Theta_{R,j}}{T_{R,j}}\right) \leq c_{S,N_0} + \sum_{j=1}^i \sum_{k=1}^K T_{S_k,j} \log\left(1 + \frac{\gamma_{S_k,R} \Theta_{S_k,j}}{T_{S_k,j}}\right), \quad \forall i, \quad (38)$$

$$p_{R,n} + q_{R,n} \leq b_{R,n-1}, \quad p_{S_k,n} \leq b_{S_k,n-1}, \quad \forall n, \quad \forall k, \quad (39)$$

$$\sum_{j=1}^i \Theta_{S_k,i} \leq b_{S_k,N_0} + \phi_{R,S_k} \sum_{j=1}^i \Theta_{R,j} - \mathbf{1}_{i=I} \cdot B_{S_k,\text{res}}, \quad \forall i, \quad \forall k, \quad (40)$$

$$\sum_{j=1}^i \Theta_{R,i} \leq b_{R,N_0} + \sum_{j=1}^i E_{R,j} - \mathbf{1}_{i=I} \cdot B_{R,\text{res}}, \quad \forall i, \quad (41)$$

$$\sum_{k=1}^K T_{S_k,i} + T_{R,i} \leq T_i, \quad \forall i, \quad (42)$$

$$g_i^{(b)}(\mathbf{p}_{R,N_0}, \mathbf{T}_{R,i}, \Theta_{R,i}) = f_{N_0}^{(b)}(\mathbf{p}_{R,N_0}) + \sum_{j=1}^i h(T_{R,j}, \Theta_{R,j}, T_{R,j}^{(b-1)}, \Theta_{R,j}^{(b-1)}), \quad (43)$$

$$h(T, \Theta, T_0, \Theta_0) = \left(\log\left(1 + \frac{\gamma_{R,D} \Theta_0}{T_0}\right) - \frac{\gamma_{R,D} \Theta_0}{T_0 + \gamma_{R,D} \Theta_0} \right) (T - T_0) + \frac{\gamma_{R,D} T_0 (\Theta - \Theta_0)}{T_0 + \gamma_{R,D} \Theta_0} + T_0 \log\left(1 + \frac{\gamma_{R,D} \Theta_0}{T_0}\right). \quad (44)$$

imated by $g_i^{(b)}(\mathbf{p}_{R,N_0}, \mathbf{T}_{R,i}, \Theta_{R,i})$ in (43), as shown at the top of this page, where we define vectors $\mathbf{T}_{R,i} = (T_{R,j})_{j=1}^i$, $\Theta_{R,i} = (\Theta_{R,j})_{j=1}^i$ and the function $h(T, \Theta, T_0, \Theta_0)$ in (44), as shown at the top of this page. Notice that for each sub-problem p , the initial values of $\mathbf{p}_{R,n}^{(0)}$, $\mathbf{T}_{R,i}^{(0)}$ and $\Theta_{R,i}^{(0)}$ can be chosen as any positive value satisfying the constraints in (P6). It has been proved in [46] that the SPCA method guarantees convergence to a KKT point of p . Details of the SPCA method to solve a sub-problem p can be found in Algorithm 4.

For the lower bound of sub-problem p , it can be estimated by deriving a feasible solution heuristically. With the obtained optimal solution to the upper bound of p , it can be exploited to produce a feasible time scheduling vector \mathbf{x}_{N-N_0} for the last $N - N_0$ unassigned time slots by rounding the continuous epochs into integers. Then, with all the N time slots being assigned by $\mathbf{x}_N = (\mathbf{x}_{N_0}, \mathbf{x}_{N-N_0})$, a feasible lower bound of sub-problem p can be derived by Algorithm 4.

B. A Sub-Optimal Offline Algorithm

Generally, the BnB framework can solve (P1) efficiently. However, its computational complexity is exponential in the worst case. Thus, we propose a sub-optimal offline algorithm.

We consider to greedily prune branches with comparatively low upper bounds, which can reduce the searching space from exponential to polynomial. This is due to the observation that the branch with a higher upper bound is more likely to lead to a better optimal system throughput. Specifically, for each $n \in \mathcal{N}$, if we define $\mathcal{P}_n \subseteq \mathcal{P}$ as the set of sub-problems of (P1) with the first n time slots being assigned, only sub-problems with the highest Y_{\max} upper bounds in \mathcal{P}_n will be reserved for further processing, while other sub-problems branches are greedily

pruned. Here, Y_{\max} is a pre-selected constant integer, and the performance of the sub-optimal offline algorithm approaches to the optimal BnB method as Y_{\max} grows. Later, we will show numerically that even small Y_{\max} can lead to results very close to the upper bound throughput. In this way, time complexity of the sub-optimal offline algorithm will be no more than $O(Y_{\max} K N^{c+1} N_{\text{itr}})$, where $O(Y_{\max} K N)$ scales the number of branches visited, $c < 3$ is a constant and $O(N^c N_{\text{itr}})$ is the time to derive the upper bound of a branch by solving (P6). Specifically, $O(N^c)$ denotes the complexity to generally solve a linearized convex optimization problem [44], and N_{itr} denotes the average number of iterations, which will be bounded by a threshold. Therefore, the sub-optimal offline algorithm can solve (P1) in polynomial time.

C. A Heuristic Online Algorithm

For the online problem of (P1), only causal information of R 's random energy arrivals is available for optimization, i.e., the current and all the previous energy arrivals. Besides, statistical information, i.e., the average EH rate of the relay node P_H , is also known. In this setup, we need to determine power allocation and time scheduling jointly for each slot during transmission.

Inspired by the optimal solution to (P3) in Algorithm 2, each node $u \in \mathcal{U}$ will attempt to transmit with a constant power as long as possible, which is denoted as the reference transmission power $\bar{P}_{u,\text{ref}}$. If the battery energy for all the nodes is insufficient to transmit at slot $n \in \mathcal{N}$, the reference powers $\{\bar{P}_{u,\text{ref}}\}_{u \in \mathcal{U}}$ need to be updated, which are calculated by regarding the transmission of the remaining $N - n + 1$ slots as a fixed energy model problem with estimated initial conditions. Thus, with the residual energy of each node $u \in \mathcal{U}$

after slot $n - 1$, i.e., $b_{u,n-1}$, we can estimate the total expected energy of R from slot n through N as

$$\bar{E}_{R,n} = b_{R,n-1} + (N - n + 1)P_H - B_{R,\text{res}}. \quad (46)$$

Similarly, the total expected RF energy of each S_k is

$$\bar{E}_{S_k,n} = b_{S_k,n-1} + \phi_{R,S_k} \bar{E}_{R,n} - B_{S_k,\text{res}}. \quad (47)$$

Meanwhile, let d_{ini} be the amount of residual data in the relay node's buffer after slot $n - 1$ and $d_{\text{res}} = 0$. Then, for each node $u \in \mathcal{U}$, the optimal transmission power $P_{u,n}^*$ can be derived by Theorem 1 with the above estimated parameters and then update the reference power by $\bar{P}_{u,\text{ref}} = P_{u,n}^*$.

With the above updating strategy, we summarize the heuristic time scheduling and power allocation algorithm for each upcoming time slot $n \in \mathcal{N}$ in the following four rules.

- 1) If slot $n = N$, it is assigned to R to transmit with $P_{R,N}^{\text{Online}} = \max\{0, b_{R,N-1} + P_H - B_{R,\text{res}}\}$.
- 2) If slot $n = 1$ or $n = n_{\text{update}}$, update the reference powers by $\bar{P}_{u,\text{ref}} = P_{u,n}^*$ for $\forall u \in \mathcal{U}$;
- 3) If any S_k has sufficient battery energy for transmission, i.e., $b_{S_k,n-1} \geq \mu \bar{P}_{S_k,\text{ref}}$, slot n will be assigned to S_k to transmit with $P_{S_k,n}^{\text{Online}} = \mu \bar{P}_{S_k,\text{ref}}$.
- 4) Otherwise, R will be selected and make the best effort to transmit with power $P_{R,n}^{\text{Online}} = \min\{\mu \bar{P}_{R,\text{ref}}, b_{R,n-1}\}$. Besides, if $\mu \bar{P}_{R,\text{ref}} < b_{R,n-1}$, set $n_{\text{update}} = n + 1$.

Here, $\mu \in (0, 1]$ is defined as the *power saving ratio* intended for conservative power control, whose effects will be discussed in numerical simulations. In the above algorithm, we prefer to choose any S_k to transmit if it has sufficient battery energy, while the last slot is reserved for R . It is also worth noting that R may forward with some extra charging power $q_{R,n+1}$ in addition to the effective transmission power $p_{R,n+1}$, which gives $P_{R,n+1}^{\text{Online}} = p_{R,n+1} + q_{R,n+1}$. According to the last three rules, all the nodes in the network will transmit with constant powers as many time slots as possible when the battery energy of R is not exhausted. After that, the reference powers will be updated and adapt to subsequent random energy arrivals. The time complexity of the online algorithm is bounded by $O(N)$, since it only needs to solve (P4) at most once for each slot to get the reference powers.

V. NUMERICAL ANALYSIS

In this section, we will conduct extensive numerical simulations to demonstrate the significance of joint time scheduling and power allocation. The performances of the upper bound derived by (P2), the proposed sub-optimal offline algorithm and the proposed heuristic online algorithm will be compared by system sum-throughput averaged by N . In the simulations, the total number of time slots $N = 60$. The channel power gain from node u to node v is modeled as $h_{u,v} = 10^{-3} d_{u,v}^{-\alpha}$, where $d_{u,v}$ is the distance in meters and $\alpha = 2.5$ is the path-loss exponent. Note that the signal power attenuation at a reference distance of 1m is 30dB and the distance between the relay node and the destination node is $d_{R,D} = 1\text{km}$. Assume the bandwidth $W = 1\text{MHz}$ and the additive white Gaussian noise at each node has a power spectral density $N_0 = 10^{-19}\text{W/Hz}$. We also assume the per-slot random energy arrival

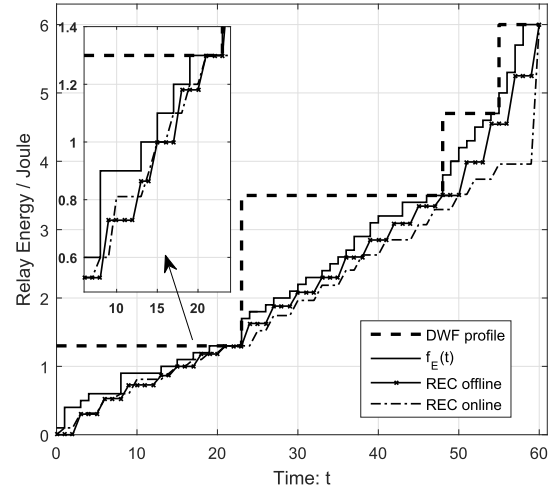


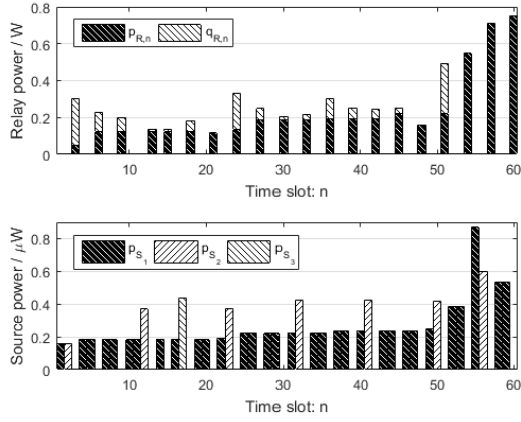
Fig. 5. Given an instance of the random energy profile represented by $f_E(t)$, illustration of the corresponding DWF energy profile, and the REC curves of the proposed offline and online algorithms, respectively.

E_n follows an i.i.d uniform distribution in $[0, 2P_H]$ and the energy conversion efficiency $\eta = 0.5$. Besides, the initial and residual energy is set to be $B_{R,\text{ini}} = B_{R,\text{res}} = P_H$ for R and $B_{S_k,\text{ini}} = B_{S_k,\text{res}} = \max_{j \in \mathcal{X}}\{\phi_{R,S_j} P_H\}$ for each S_k . In order to keep sufficiently low complexity but good performance, we choose $Y_{\text{max}} = 2$ for the sub-optimal offline algorithm.

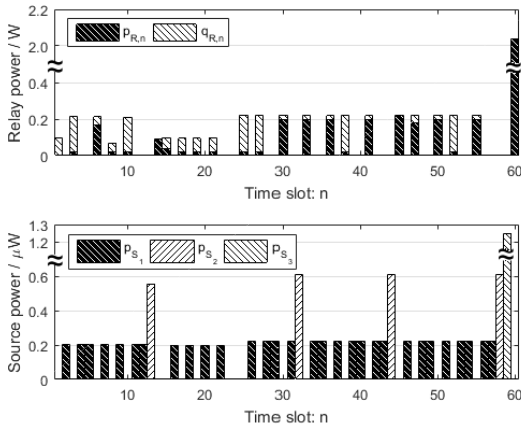
A. Illustration of Joint Time Scheduling and Power Allocation

By assuming the average EH rate of the relay node $P_H = 0.1\text{W}$, we can obtain an instance of the random energy profile $\{E_n\}_{n=1}^N$, from which we can derive the total available energy curve $f_E(t)$ as well as the corresponding DWF energy profile, as shown in Fig. 5. Then, the optimal solutions can be derived using the proposed offline and online algorithms, which gives the accumulative energy consumption curves of the relay node as *REC offline* and *REC online*, respectively. Note that $\mu = 0.72$ is set for the online algorithm. Being constrained by the $f_E(t)$ curve, it can be seen that both the offline and online curves can track the $f_E(t)$ curve, where the gap for the offline curve is much smaller than the online curve, especially for the increasing gap during the last half of time slots.

The assignments of time slots along with associated power allocations for the two algorithms are also presented in Fig. 6(a) and Fig. 6(b), respectively. We can observe that although the number of slots assigned to the relay node in the offline algorithm is less than that of the online algorithm, the proportion of the effective transmission power to the overall relay power at each slot is much higher, which not only spares more slots to the source nodes for data transmission to the relay node, but also improves the forwarding throughput of the relay node and thus the resulting system sum-throughput. Therefore, we know that both the offline and online algorithms can schedule slots and allocate power levels adaptively to the random energy profile. Additionally, using non-causal energy information, the offline algorithm can fit the random energy arrivals much better and utilize the harvested energy more efficiently.



(a) Results of the offline algorithm for all the source and relay nodes, given the random energy profile in Fig. 5.



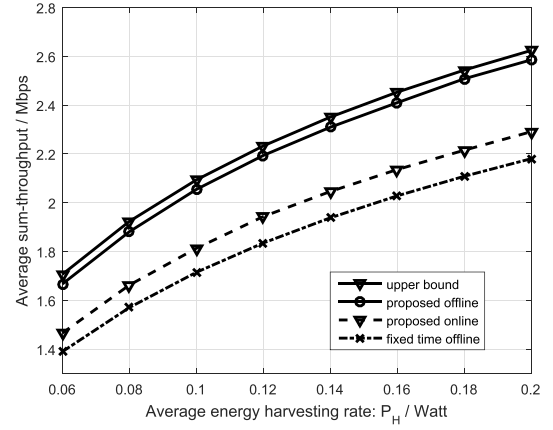
(b) Results of the online algorithm for all the source and relay nodes, given the random energy profile in Fig. 5.

Fig. 6. Illustration of the optimal time scheduling and power allocation by the offline and online algorithms.

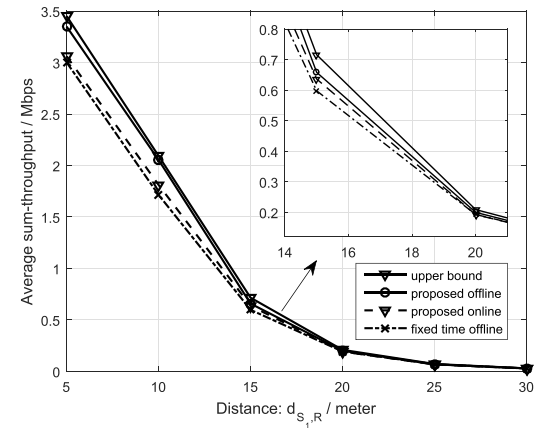
B. Evaluation of System Sum-Throughput Performance

To compare the throughput performance of the proposed offline and online algorithms, we consider the *fixed time offline* power allocation strategy in [38] as a baseline scheme, which employs offline power allocation for a fixed and equal time scheduling by alternative sending and forwarding.

We first investigate the average sum-throughput for a single source nodes system, i.e., $K = 1$. In Fig. 7(a), all the throughput curves are concave functions in terms of P_H , where both the proposed offline and online algorithms outperform the fixed time scheduling scheme significantly. Thus, it demonstrates the importance of proper time scheduling according to the channel and energy state for each node. Besides, the performance gap between the proposed offline algorithm and the upper bound is very small, which verifies the efficiency of the sub-optimal offline algorithm. In Fig. 7(b), the throughput decrease dramatically as the distance of the source node to the relay node $d_{S_1,R}$ increases, which indicates the wireless energy charging efficiency is highly impacted by the path loss. Therefore, we consider a charging distance within 20 meters in other experiments.



(a) Distance $d_{S_1,R} = 10$ meters and the power saving ratio $\mu = 0.9$ for the online algorithm.



(b) The relay node's EH rate $P_H = 0.1W$ and the power saving ratio $\mu = 0.9$ for the online algorithm.

Fig. 7. Average sum-throughputs versus the EH rate P_H and the distance $d_{S_1,R}$ for a single source nodes system.

As for a system with multiple source nodes, we assume that each source node S_k is uniformly located in a distance of 10 to 20 meters to the relay node R , i.e., $d_{S_k,R} = 10 + \frac{10}{K-1} \cdot (k-1)$ for $k \in \mathcal{K}$. In Fig. 8, the system sum-throughput is illustrated for a $K = 5$ source nodes system, which is similar to the single source node case in Fig. 7(a). Moreover, we also examine system performance for different number of source nodes in Fig. 9. It can be observed that the system sum-throughput increases as the number of source nodes K grows, since more RF energy is harvested by a larger set of source nodes and thus more source bits can be transmitted to R . However, it comes with the decrease of the individual throughput for each source node. Moreover, it is worth noting that the throughput gap between the proposed offline algorithm and the upper bound is very small, despite the slight increase for very large K 's. As for the online algorithm, although the gap to the upper bound is much smaller than that of the fixed time offline algorithm for smaller K 's, the gap increases when more source nodes come in, since it is more challenging to online schedule time slots and allocate transmission powers for more users.

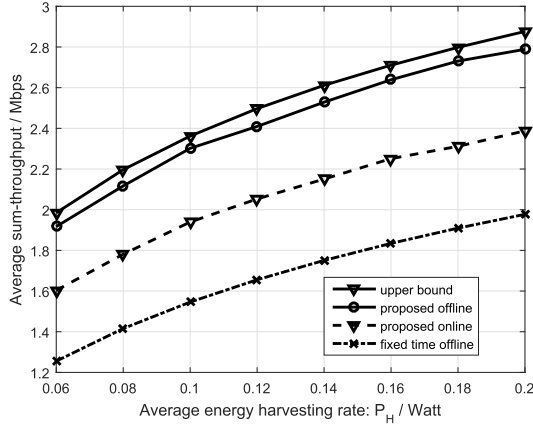


Fig. 8. Average sum-throughput for a $K = 5$ source nodes system. The distances $d_{S_k,R} = 10, 12.5, 15, 17.5, 20$ meters, respectively, and $\mu = 0.76$ for the online algorithm.

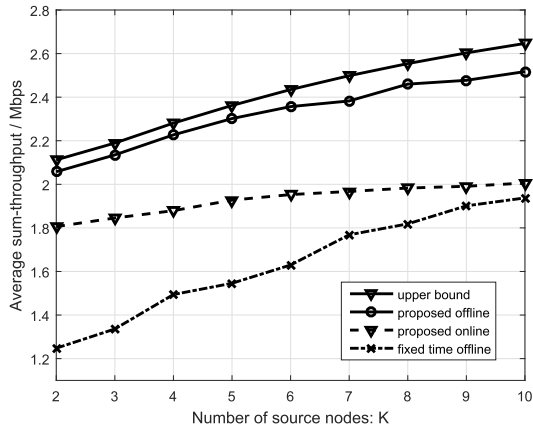


Fig. 9. Average sum-throughput versus the number of the source nodes K . Here, $P_H = 0.1W$ and μ is optimized for different K respectively in the online algorithm.

To enhance the online algorithm, we observe that transmitting with full reference power may increase the power threshold and also deplete the source nodes' battery energy much faster, which leads to less time slots to be assigned to the source nodes and lower system throughput. Thus, we consider to conservatively allocate the transmission power and find out that there exists one optimal power saving ratio μ for a given number of source nodes K , as shown in Fig. 10. Moreover, it can be seen that the optimal μ decreases as K grows.

We finally study the connection between the average sum-throughput and the number of time slots N in Fig. 11. It can be observed that for all cases, the average throughput performances increase as the number of time slots N grows, regardless of the number of source nodes K . This is because for a smaller N , the randomness of the energy arrivals $\{E_n\}_{n=1}^N$ will lead to a much less balanced power allocation for each time slot, which results in a lower average throughput. Moreover, the performance gaps of both the proposed offline and online algorithms to the upper bound become smaller for a larger N . However, compared with the proposed offline algorithms, the performance of the online algorithm is quite

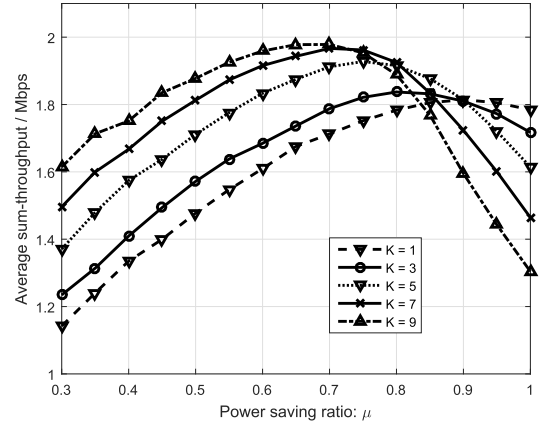


Fig. 10. Average sum-throughput of the proposed online algorithm versus the power saving ratio μ . Here, the average EH rate $P_H = 0.1W$.

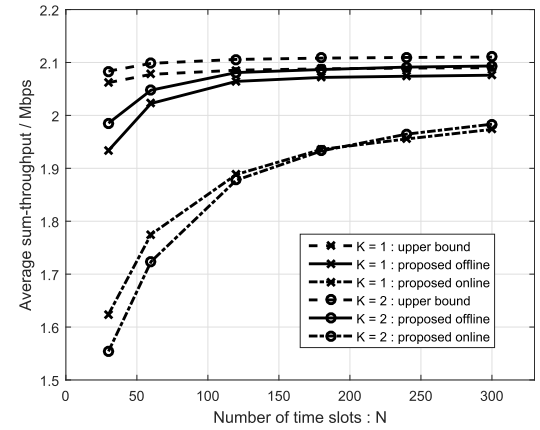


Fig. 11. Average sum-throughput versus the number of the time slots N . The average EH rate $P_H = 0.1W$ and $\mu = 1$ for both the $K = 1$ and $K = 2$ cases in the online algorithm.

low for smaller N 's. This is due to the fact that it only requires causal information of the network system, which will significantly lower down the system throughput. Nevertheless, the gap for the online algorithm will shrink dramatically as N grows. Therefore, we know that the randomness of the energy arrivals have much higher impact on the system performance for smaller N 's, especially for the online algorithm.

VI. CONCLUSION

In this paper, we have studied a fully sustainable wireless cooperative communication network, where the relay node utilizes its harvested green energy to support not only data transmission to the destination node, but also RF energy charging for all the source nodes. A system sum-throughput maximization problem is formulated to jointly optimize time scheduling and power allocation over a finite time horizon. To solve the problem, we firstly analyze its upper bound by relaxation and then propose an optimal BnB framework, which can be extended to an efficient sub-optimal offline algorithm as well as a heuristic online algorithm. The superiority of the proposed algorithms are verified by numerical simulations, which shows the sub-optimal algorithm approaches the upper bound with polynomial time complexity.

APPENDIX
PROOF OF THEOREM 1

Proof: Let $g(T_S)$ be the optimum of the following convex throughput maximization problem,

$$\max_{T_{S_k} \geq 0, \sum_{k=1}^K T_{S_k} \leq T_S} \sum_{k=1}^K T_{S_k} \log\left(1 + \frac{\gamma_{S_k, R} E_{S_k}}{T_{S_k}}\right), \quad (48)$$

which can be solved by KKT conditions in closed form. Let vector $\mathbf{T} = (T_{S_1}, T_{S_2}, \dots, T_{S_K})$. The Lagrangian function can be written by $\mathcal{L}(\mathbf{T}, \lambda) = \sum_{k=1}^K T_{S_k} \log\left(1 + \frac{\gamma_{S_k, R} E_{S_k}}{T_{S_k}}\right) - \lambda (\sum_{k=1}^K T_{S_k} - T_S)$ for the multiplier $\lambda \geq 0$. Differentiating the Lagrangian function with respect to T_{S_k} , we obtain

$$\frac{\partial \mathcal{L}}{\partial T_{S_k}} = \log\left(1 + \frac{\gamma_{S_k, R} E_{S_k}}{T_{S_k}}\right) - \frac{\gamma_{S_k, R} E_{S_k}}{T_{S_k} + \gamma_{S_k, R} E_{S_k}} - \lambda = 0. \quad (49)$$

The optimal dual variable λ^* satisfies KKT condition $\lambda^* (\sum_{k=1}^K T_{S_k} - T_S) = 0$. Assume that $\lambda^* > 0$. If we define the function $h(x) = \log(1+x) - \frac{x}{1+x}$, from (49) we have

$$h\left(\frac{\gamma_{S_k, R} E_{S_k}}{T_{S_k}^*}\right) = \lambda^*, \quad \forall k \in \mathcal{K}. \quad (50)$$

It can be verified that $h(x)$ is monotonically increasing of $x \geq 0$. Therefore, from (50) we know that $\frac{\gamma_{S_1, R} E_{S_1}}{T_{S_1}^*} = \frac{\gamma_{S_2, R} E_{S_2}}{T_{S_2}^*} = \dots = \frac{\gamma_{S_K, R} E_{S_K}}{T_{S_K}^*}$. Considering $\sum_{k=1}^K T_{S_k}^* = T_S$, we have

$$T_{S_k}^* = T_S \cdot \frac{\gamma_{S_k, R} E_{S_k}}{\sum_{j=1}^K \gamma_{S_j, R} E_{S_j}}, \quad \forall k \in \mathcal{K}. \quad (51)$$

If we denote $f(T_R) = T_R \log\left(1 + \frac{\gamma_{R, D} E_R}{T_R}\right)$, the two functions $f(T_R)$ and $g(T_S)$ are monotonically increasing function of T_R and T_S , respectively. Thus, the maximum of (P4) can be obtained by letting $f(T_R) = d_0 + g(T - T_R) - d_M$, which gives the equation (24) in Theorem 1. The root of (24) can be efficiently solved by numerical algorithms and gives the optimal value of T_R^* . Finally, with $T_S^* = T - T_R^*$, the optimal values of $T_{S_k}^*$ can be derived from (51). \square

APPENDIX
PROOF OF LEMMA 2

Proof: Suppose that in the optimal solution, the average power of the relay node R may decrease for some rounds. Thus, there must be two successive rounds m and $m+1$ satisfying $P_{R, m}^{\text{avg}} > P_{R, m+1}^{\text{avg}}$. According to the definition in (27), we have $\frac{\bar{P}_{R, m} \tau_{R, m}}{\sum_{k=1}^K \tau_{S_k, m} + \tau_{R, m}} > \frac{\bar{P}_{R, m+1} \tau_{R, m+1}}{\sum_{k=1}^K \tau_{S_k, m+1} + \tau_{R, m+1}}$. The total energy consumed by the relay node during these two rounds can be derived by $E_R = \bar{P}_{R, m} \tau_{R, m} + \bar{P}_{R, m+1} \tau_{R, m+1}$. With keeping all the initial and residual states of the sources and relay, sum-throughput maximization of the two rounds can be formulated as a problem of (P3) with given fixed total available energy of the relay node E_R . As a result, according to Theorem 2 and (27), there exists an optimal solution that the average powers of R for these two rounds are optimized to be constant as $P_{R, m}^{\text{avg}} = P_{R, m+1}^{\text{avg}} = \frac{\bar{P}_{R, m} \tau_{R, m} + \bar{P}_{R, m+1} \tau_{R, m+1}}{\sum_{k=1}^K \tau_{S_k, m} + \tau_{R, m} + \sum_{k=1}^K \tau_{S_k, m+1} + \tau_{R, m+1}}$, which suggests that the

sum-throughput will not decrease for any round and we can always find an optimal solution with non-decreasing average power of the relay node R . \square

APPENDIX
PROOF OF LEMMA 3

Proof: Suppose the optimal AEC curve ever arrives at a point on the left of the AEC_B curve. Given the random energy arrivals, the relay node must decrease its average power and grow across the AEC_B curve at some subsequent rounds, otherwise its energy consumption will exceed the total available energy $f_E(t)$ and violate the energy causality constraints. Thus, the slope of the assumed AEC curve is not always non-decreasing, which contradicts with Lemma 2. Therefore, we know that the optimal AEC curve never grows on the left side of the AEC_B curve. \square

REFERENCES

- [1] L. X. Cai, Y. Liu, T. H. Luan, X. Shen, J. W. Mark, and H. V. Poor, "Sustainability analysis and resource management for wireless mesh networks with renewable energy supplies," *IEEE J. Sel. Area Commun.*, vol. 32, no. 2, pp. 345–355, Feb. 2014.
- [2] G. Piro *et al.*, "HetNets powered by renewable energy sources: Sustainable next-generation cellular networks," *IEEE Internet Comput.*, vol. 17, no. 1, pp. 32–39, Jan./Feb. 2013.
- [3] X. Huang and N. Ansari, "Energy sharing within EH-enabled wireless communication networks," *IEEE Wireless Commun.*, vol. 22, no. 3, pp. 144–149, Jun. 2015.
- [4] X. Huang, T. Han, and N. Ansari, "On green-energy-powered cognitive radio networks," *IEEE Commun. Surveys Tuts.*, vol. 17, no. 2, pp. 827–842, 2nd Quart., 2015.
- [5] X. Huang, T. Han, and N. Ansari, "Smart grid enabled mobile networks: Jointly optimizing bs operation and power distribution," *IEEE/ACM Trans. Netw.*, vol. 25, no. 3, pp. 1832–1845, Jun. 2017.
- [6] S. Ulukus *et al.*, "Energy harvesting wireless communications: A review of recent advances," *IEEE J. Sel. Areas Commun.*, vol. 33, no. 3, pp. 360–381, Mar. 2015.
- [7] J. Yang and S. Ulukus, "Optimal packet scheduling in an energy harvesting communication system," *IEEE Trans. Commun.*, vol. 60, no. 1, pp. 220–230, Jan. 2012.
- [8] C. K. Ho and R. Zhang, "Optimal energy allocation for wireless communications with energy harvesting constraints," *IEEE Trans. Signal Process.*, vol. 60, no. 9, pp. 4808–4818, Sep. 2012.
- [9] O. Ozel, K. Tutuncuoglu, J. Yang, S. Ulukus, and A. Yener, "Transmission with energy harvesting nodes in fading wireless channels: Optimal policies," *IEEE J. Sel. Areas Commun.*, vol. 29, no. 8, pp. 1732–1743, Sep. 2011.
- [10] Y. Luo, J. Zhang, and K. B. Letaief, "Optimal scheduling and power allocation for two-hop energy harvesting communication systems," *IEEE Trans. Commun.*, vol. 12, no. 9, pp. 4729–4741, Sep. 2013.
- [11] O. Orhan and E. Erkip, "Energy harvesting two-hop communication networks," *IEEE J. Sel. Area Commun.*, vol. 33, no. 12, pp. 2658–2670, Dec. 2015.
- [12] C. Huang, R. Zhang, and S. Cui, "Throughput maximization for the Gaussian relay channel with energy harvesting constraints," *IEEE J. Sel. Areas Commun.*, vol. 31, no. 8, pp. 1469–1479, Aug. 2013.
- [13] X. Lu, P. Wang, D. Niyato, D. I. Kim, and Z. Han, "Wireless charging technologies: Fundamentals, standards, and network applications," *IEEE Commun. Surveys Tuts.*, vol. 18, no. 2, pp. 1413–1452, 2nd Quart., 2015.
- [14] F. Zhao, L. Wei, and H. Chen, "Optimal time allocation for wireless information and power transfer in wireless powered communication systems," *IEEE Trans. Veh. Technol.*, vol. 65, no. 3, pp. 1830–1835, Mar. 2016.
- [15] H. Ju and R. Zhang, "Throughput maximization in wireless powered communication networks," *IEEE Trans. Wireless Commun.*, vol. 13, no. 1, pp. 418–428, Jan. 2014.
- [16] K. Huang and V. K. N. Lau, "Enabling wireless power transfer in cellular networks: Architecture, modeling and deployment," *IEEE Trans. Wireless Commun.*, vol. 13, no. 2, pp. 902–912, Feb. 2014.

- [17] G. Yang, C. K. Ho, and Y. L. Guan, "Dynamic resource allocation for multiple-antenna wireless power transfer," *IEEE Trans. Signal Process.*, vol. 62, no. 14, pp. 3565–3577, Jul. 2014.
- [18] P. Grover and A. Sahai, "Shannon meets tesla: Wireless information and power transfer," in *Proc. IEEE Int. Symp. Inf. Theory (ISIT)*, Jun. 2010, pp. 2363–2367.
- [19] D. N. K. Jayakody, J. Thompson, S. Chatzinotas, and S. Durrani, *Wireless Information and Power Transfer: A New Green Communications Paradigm*. New York, NY, USA: Springer-Verlag, Apr. 2017.
- [20] X. Zhou, R. Zhang, and C. K. Ho, "Wireless information and power transfer: Architecture design and rate-energy tradeoff," *IEEE Trans. Commun.*, vol. 61, no. 11, pp. 4754–4767, Nov. 2013.
- [21] G. L. Moritz, J. L. Rebelatto, R. D. Souza, B. Uchôa-Filho, and Y. Li, "Time-switching uplink network-coded cooperative communication with downlink energy transfer," *IEEE Trans. Signal Process.*, vol. 62, no. 19, pp. 5009–5019, Oct. 2014.
- [22] S. Timotheou, I. Krikidis, G. Zheng, and B. Ottersten, "Beamforming for MISO interference channels with QoS and RF energy transfer," *IEEE Trans. Wireless Commun.*, vol. 13, no. 5, pp. 2646–2658, May 2014.
- [23] A. Rajaram, D. N. K. Jayakody, K. Srinivasan, B. Chen, and V. Sharma, "Opportunistic-harvesting: RF wireless power transfer scheme for multiple access relays system," *IEEE Access*, vol. 5, pp. 16084–16099, 2017.
- [24] X. Chen, Z. Zhang, H.-H. Chen, and H. Zhang, "Enhancing wireless information and power transfer by exploiting multi-antenna techniques," *IEEE Commun. Mag.*, vol. 53, no. 4, pp. 133–141, Apr. 2015.
- [25] Z. Ding *et al.*, "Application of smart antenna technologies in simultaneous wireless information and power transfer," *IEEE Commun. Mag.*, vol. 53, no. 4, pp. 86–93, Apr. 2015.
- [26] Z. Chen, Z. Chen, L. X. Cai, and Y. Cheng, "Energy-throughput tradeoff in sustainable cloud-RAN with energy harvesting," in *Proc. IEEE Int. Conf. Commun. (ICC)*, May 2017, pp. 1–6.
- [27] J. Xu, L. Liu, and R. Zhang, "Multiuser MISO beamforming for simultaneous wireless information and power transfer," *IEEE Trans. Signal Process.*, vol. 62, no. 18, pp. 4798–4810, Sep. 2014.
- [28] R. Morsi, D. S. Michalopoulos, and R. Schober, "Multiuser scheduling schemes for simultaneous wireless information and power transfer over fading channels," *IEEE Trans. Wireless Commun.*, vol. 14, no. 4, pp. 1967–1982, Apr. 2015.
- [29] Z. Xiang and M. Tao, "Robust beamforming for wireless information and power transmission," *IEEE Wireless Commun. Lett.*, vol. 1, no. 4, pp. 372–375, Aug. 2012.
- [30] R. Zhang and C. K. Ho, "MIMO broadcasting for simultaneous wireless information and power transfer," *IEEE Trans. Wireless Commun.*, vol. 12, no. 5, pp. 1989–2001, May 2013.
- [31] X. Chen, C. Yuen, and Z. Zhang, "Wireless energy and information transfer tradeoff for limited-feedback multi-antenna systems with energy beamforming," *IEEE Trans. Veh. Technol.*, vol. 63, no. 1, pp. 407–412, Jan. 2014.
- [32] L. Liu, R. Zhang, and K.-C. Chua, "Wireless information transfer with opportunistic energy harvesting," *IEEE Trans. Wireless Commun.*, vol. 12, no. 1, pp. 288–300, Jan. 2013.
- [33] S. Lee, R. Zhang, and K. Huang, "Opportunistic wireless energy harvesting in cognitive radio networks," *IEEE Trans. Wireless Commun.*, vol. 12, no. 9, pp. 4788–4799, Sep. 2013.
- [34] I. Krikidis, S. Timotheou, and S. Sasaki, "RF energy transfer for cooperative networks: Data relaying or energy harvesting?" *IEEE Commun. Lett.*, vol. 16, no. 11, pp. 1772–1775, Nov. 2012.
- [35] A. A. Nasir, X. Zhou, S. Durrani, and R. A. Kennedy, "Wireless-powered relays in cooperative communications: Time-switching relaying protocols and throughput analysis," *IEEE Trans. Commun.*, vol. 63, no. 5, pp. 1607–1622, May 2015.
- [36] Z. Ding, S. M. Perlaza, I. Esnaola, and H. V. Poor, "Power allocation strategies in energy harvesting wireless cooperative networks," *IEEE Trans. Wireless Commun.*, vol. 13, no. 2, pp. 846–860, Feb. 2014.
- [37] H. Chen, Y. Li, J. L. Rebelatto, B. F. Uchôa-Filho, and B. Vucetic, "Harvest-then-cooperate: Wireless-powered cooperative communications," *IEEE Trans. Signal Process.*, vol. 63, no. 7, pp. 1700–1711, Apr. 2015.
- [38] X. Huang and N. Ansari, "Optimal cooperative power allocation for energy-harvesting-enabled relay networks," *IEEE Trans. Veh. Technol.*, vol. 65, no. 4, pp. 2424–2434, Apr. 2016.
- [39] S. Luo, G. Yang, and K. C. Teh, "Throughput of wireless-powered relaying systems with buffer-aided hybrid relay," *IEEE Trans. Wireless Commun.*, vol. 15, no. 7, pp. 4790–4801, Jul. 2016.
- [40] A. Rajaram, D. N. K. Jayakody, and V. Skachek, "Store-then-cooperate: Energy harvesting scheme in cooperative relay networks," in *Proc. Int. Symp. Wireless Commun. Syst. (ISWCS)*, Sep. 2016, pp. 445–450.
- [41] N. Zlatanov, R. Schober, and P. Popovski, "Buffer-aided relaying with adaptive link selection," *IEEE J. Sel. Areas Commun.*, vol. 31, no. 8, pp. 1530–1542, Aug. 2013.
- [42] I. Ahmed, A. Ikhlef, R. Schober, and R. K. Mallik, "Power allocation for conventional and buffer-aided link adaptive relaying systems with energy harvesting nodes," *IEEE Trans. Wireless Commun.*, vol. 13, no. 3, pp. 1182–1195, Mar. 2014.
- [43] X. Huang and N. Ansari, "Data and energy cooperation in relay-enhanced ofdm systems," in *Proc. IEEE Int. Conf. Commun. (ICC)*, May 2016, pp. 1–6.
- [44] S. Boyd and L. Vandenberghe, *Convex Optimization*. Cambridge, U.K.: Cambridge Univ. Press, 2004.
- [45] R. M. Corless, G. H. Gonnet, D. E. G. Hare, D. J. Jeffrey, and D. E. Knuth, "On the LambertW function," *Adv. Comput. Math.*, vol. 5, no. 1, pp. 329–359, 1996.
- [46] A. Beck, A. Ben-Tal, and L. Tetrushvili, "A sequential parametric convex approximation method with applications to nonconvex truss topology design problems," *J. Global Optim.*, vol. 47, no. 1, pp. 29–51, 2010.
- [47] P. Belotti, J. Lee, L. Liberti, F. Margot, and A. Wächter, "Branching and bounds tightening techniques for non-convex MINLP," *Optim. Methods Softw.*, vol. 24, nos. 4–5, pp. 597–634, 2009.



Zhao Chen received the B.S. and Ph.D. degrees in electronic engineering from Tsinghua University, Beijing, China, in 2010 and 2015, respectively. He is currently a Post-Doctoral Research Fellow with the Department of Electrical and Computer Engineering, Illinois Institute of Technology, Chicago, IL, USA. His research interests include resource allocation, cross-layer design, energy harvesting, and stochastic geometry in wireless communications and networking.



Lin X. Cai received the M.A.Sc. and Ph.D. degrees in electrical and computer engineering from the University of Waterloo, Waterloo, Canada, in 2005 and 2010, respectively. She was a Post-Doctoral Research Fellow with the Electrical Engineering Department, Princeton University, in 2011. She joined the Huawei US Wireless Research and Development Center in 2012 as a Senior Engineer. She has been an Assistant Professor with the Department of Electrical and Computer Engineering, Illinois Institute of Technology, Chicago, IL, USA, since 2014. Her research interests include green communication and networking, broadband multimedia services, and radio resource and mobility management. She received a Postdoctoral Fellowship Award from the Natural Sciences and Engineering Research Council of Canada in 2010, a Best Paper Award from the IEEE Globecom 2011, and an NSF Career Award in 2016. She is an Associate Editor for the *IEEE Network Magazine*, and a co-chair for the IEEE conferences.



Yu Cheng (S'01–M'04–SM'09) received B.E. and M.E. degrees in electrical engineering from Tsinghua University in 1995 and 1998, respectively, and the Ph.D. degree in electrical and computer engineering from the University of Waterloo, Canada, in 2003. He is currently a Full Professor with the Department of Electrical and Computer Engineering, Illinois Institute of Technology. His research interests include wireless network performance analysis, network security, big data, and cloud computing. He received a Best Paper Award at QShine 2007,

IEEE ICC 2011, and a Runner-Up Best Paper Award at ACM MobiHoc 2014. He received the National Science Foundation CAREER Award in 2011 and IIT Sigma Xi Research Award in the Junior Faculty Division in 2013. He has served as Symposium Co-Chair for the IEEE ICC and the IEEE GLOBECOM, and Technical Program Committee Co-Chair for WASA 2011, and ICNC 2015. He is a Founding Vice Chair of the IEEE ComSoc Technical Subcommittee on Green Communications and Computing. He is an IEEE ComSoc Distinguished Lecturer. He is an Associate Editor for the IEEE TRANSACTIONS ON VEHICULAR TECHNOLOGY.



Hangguan Shan (M'10) received the B.Sc. degree in electrical engineering from Zhejiang University, Hangzhou, China, in 2004, and the Ph.D. degree in electrical engineering from Fudan University, Shanghai, China, in 2009. From 2009 to 2010, he was a Post-Doctoral Research Fellow with the University of Waterloo, Waterloo, ON, Canada. Since 2011, he has been with the College of Information Science and Electronic Engineering, Zhejiang University, where he is currently an Associate Professor. His current research focuses on cross-layer protocol

design, resource allocation, and the quality-of-service provisioning in wireless networks. He is a co-recipient of the Best Industry Paper Award from the 2011 IEEE WCNC. He has served on the Technical Program Committee as a member in various international conferences, including the IEEE Globecom, the ICC, the WCNC, and the VTC. He serves as the Track Leading Co-Chair of Future Trends and Emerging Technologies Track of the IEEE VTC 2017-Fall and has served as a Track Co-Chair of Green Communications and Networks Track of the IEEE VTC 2016-Fall. He also served as the Publicity Co-Chair for the Third and Fourth IEEE International Workshop on Wireless Sensor, Actuator, Robot Networks, and the Fifth International Conference on Wireless Communications and Signal Processing. He is currently an Editor of the IEEE TRANSACTIONS ON GREEN COMMUNICATIONS AND NETWORKING.